DOI 10.1007/s11182-014-0352-1

Russian Physics Journal, Vol. 57, No. 8, December, 2014 (Russian Original No. 8, August, 2014)

FEATURES OF MULTISTAGE THERMOELASTIC *B*2–*R*–*B*19′ MARTENSITIC TRANSFORMATIONS IN HETEROPHASE SINGLE CRYSTALS OF Ti–Ni ALLOYS

E. Yu. Panchenko,[1] Yu. I. Chumlyakov,[1] and H. Maier[2]

UDC 669.24'295-620.181:548.55

In heterophase $Ti_{50.0-x}Ni_{50.0+x}$ *(x = 0.8–1.0 at.%) single crystals after aging at 823 K for 1.5 h at the heating/cooling rate (15 ± 1) K/min and stepwise aging at 823 K for 1.5 h plus aging at 573–623 K for 1 h, multi-stage martensitic transformations are observed: there are three peaks of heat release in the DSC (differential scanning calorimetry) curves. The first peak is associated with a B2–R-transformation and increased electrical resistance ρ and the other two correspond to the development of an R–B19′-martensitic transformation occurring in two stages, and are followed by a two-stage drop of electrical resistance in the ρ(T) plot. The high-temperature stage of the R–B19′-martensitic transition is associated with transformations under the action of local stress fields in the vicinity of disperse* Ti_3Ni_4 *particles measuring ~400 nm, while the low-temperature stage is associated with transformations in the spaces between large particles containing fine disperse β′-phase particles isostructural with respect to the matrix, measuring 3–5 nm, which are formed during slow cooling from 823 K or in the course of low-temperature aging at 573–623 K.*

Keywords: thermoelastic martensitic transformations, single crystals, disperse particles.

INTRODUCTION

It is well known [1–3] that precipitation of disperse Ti_3Ni_4 particles in the aged Ti–Ni (C_{Ni} > 50.5 at.%) alloys results in the development of a martensitic transformation (MT) from the high-temperature *B*2-phase into the monoclinic *B*19′-martensite via an intermediate rhombohedral *R*-phase. It was experimentally demonstrated [2, 4–13] that in Ti–Ni alloys one can observe multistage MTs (MSMTs) during which *B*2–*R*- and *R*–*B*19′-transformations occur in a few stages: there are frequently three or sometimes four heat release peaks in the DSC (differential scanning calorimetry) curves under cooling. An X-ray or TEM examination of binary Ti–Ni alloys revealed no other phases but *B*2, *R* and *B*19′ [1, 2, 4, 5], therefore the evolution of MSMTs is attributed to the features of formation of *R*- and *B*19′-martensite in inhomogeneous materials. Primarily, an MSMT can be induced both in equiatomic Ti–Ni alloys and in those rich in Ni via thermomechanical treatment: deformation in the martensitic state followed by annealing and thermal cycling through an interval of martensitic transformations [5–7] Secondly, MSMTs are often observed in the aged Ti–Ni (C_{Ni} > 50.5 at.%) alloys under the following aging regimes: T = 723–823 K, t = 3–10 h [4, 8–11]. Within the recent fifteen years MSMTs have been extensively investigated [2, 4–13], and the available literature reports a number of approaches to interpret their physical nature, which are associated with the formation of various inhomogeneities in the Ti–Ni alloys. It has been assumed that the reasons for MSMTs in the aged binary Ti–Ni alloys could be the following: first, non-uniform distribution of nickel concentration in the space between the particles following precipitation of disperse Ti_3Ni_4 particles [4, 8, 14]. Second, it could be the presence of elastic stress fields in the vicinity of disperse particles, which are generated due to the differences in the lattice and matrix parameters [10]. Third, in more

[1]V. D. Kuznetsov Siberian Physical Technical Institute at Tomsk State University, Tomsk, Russia, [2]Leibniz University of Materials Science, Hannover, Germany, e-mail: panchenko@mail.tsu.ru. Translated from Izvestiya Vysshikh Uchebnykh Zavedenii, Fizika, No. 8, pp. 100–108, August, 2014. Original article submitted May 30 2014.

recent works G. Fan et al. [2, 12] demonstrated the occurrence of MSMTs in polycrystalline $Ti_{49.4}Ni_{50.6}$ specimens aged at 723 K for 1–24 h, while in single crystals of the same composition $Ti_{49.4}Ni_{50.6}$ aged at the above conditions no MSMTs are observed. Based on the investigations of microstructure of polycrystals undergoing MSMTs, a conclusion was made in [12] that MSMTs are caused by non-uniform distribution of particles in the material, which is associated with the presence of grain boundaries. In the course of aging of Ti–Ni polycrystals, there is a predominating precipitation of Ti_3Ni_4 particles whose size could be smaller than that in the bulk of the grain [2, 9, 11–13], which results in the development of a *B*2–(*R*)–*B*19′ MT within different temperature intervals and a manifestation of an MSMT.

In our earlier works we did not observe any MSMTs on Ti–Ni single crystals aged at $T = 673$–823 K for $t = 1$–1.5 h in a helium environment accompanied by fast heating and followed by quenching in water [15, 16]. On the other hand, MSMTs appeared in Ti–Ni (C_{Ni} = 50.8–51.0 at.%) single crystals during their aging in a vacuum setup under a constant load and in free state at $T = 823$ K, $t = 1.5$ h [3, 17, 18]. The physical cause of MSMTs was not, however, analyzed in the cited works. Neither there is an answer to the question why MSMTs are not always observed in the aged single crystals of binary Ti-Ni alloys in the cases of similar aging conditions, size range of Ti_3Ni_4 particles and interparticle spacing [12, 15–19]. The difference in the heat treatment modes during aging of Ti–Ni single crystals in free state, which is followed by quenching in water and in a vacuum setup, is associated with different cooling rates. So far there has been no analysis of the effect of heating and cooling rates during aging on the development of a *B*2–*R*–*B*19′ MT and microstructure of the aged single crystals. It was experimentally shown in [3] that in Ti–Ni (C_{Ni} = 51–52 at.%) alloys under low-temperature aging (T = 250 K, t = 1–2 h, T = 300–350 K, t = 0.1–0.5 h) equiaxial, highly dispersed β′-particles rich in nickel are formed, which are isostructural and coherent with respect to the *B*2-matrix. It is assumed that these particles can precipitate in the *B*2-phase of high-nickel Ti–Ni alloys during slow cooling from the aging temperature $T = 773$–823 K under conditions of high (more than 50.5 at.%) residual Ni concentration. These β′-phase particles, as well as the matrix, can undergo MTs, but in so doing they considerably increase the energy dissipation during transformation and the force of resistance in the course of motion of twinning boundaries in the martensite and cause MSMTs. Currently, there are no available data in the literature on the effect of these particles on the evolution of MTs in Ti–Ni alloys. Based on the above, in order to get an insight into the physical nature of MSMTs in this work we performed investigations of the development of thermoelastic *B*2–*R*–*B*19′ MTs under cooling/heating conditions in $Ti_{50.0-x}Ni_{50.0+x}$ (x = 0.8–1.0 at.%) single crystals aged at 773–823 K within 1–17 hours.

1. EXPERIMENTAL PROCEDURE

Single crystals of $Ti_{50.0-x}Ni_{50.0+x}$ (x = 0.8–1.0 at.%) were grown by the Bridgeman method in the inert gas atmosphere. In order to achieve their single-phase state, the specimens measuring 3.0 × 1.5 × 16 mm were homogenized at 1173 K for 20 h in helium at 1203 K for 0.5 h. Prior to testing, the specimens were ground and electrolythically polished in a mixture of 5% $HClO_4$ + 95% CH_3COOH at $T = 293$ K, $U = 22$ V.

Aging was performed at $T = 773$–823 K during $t = 1$–1.5 h in a vacuum setup at the heating/cooling rate (15 ± 1) K/min. The modes of aging were selected to allow measuring the particle size d from 100 to 450 nm and the interpaticle spacing λ from 100 to 400 nm [15].

The start and finish temperatures of the direct MT (M_s, M_f) and reverse MT (A_s, A_f) were determined from the variation in the electrical resistance of the specimens during the heating/cooling cycle and by the DSC method at the heating/cooling rate 10 K/min.

The microstructure of the specimens was examined in the Philips CM 200 transmission electron microscope at the accelerating voltage 200 kV. The foils for TEM examinations were prepared by spray polishing in the electrolyte 20% H_2SO_4 + 80% CH_3OH. Mechanical tests were performed in a modified Polani installation at the strain rate $\dot{\varepsilon} = 4 \cdot 10^{-4}\,1/\mathrm{s}$. The specimen orientation was determined in a Dron-3 X-Ray diffractometer using Fek_α-shell emission.

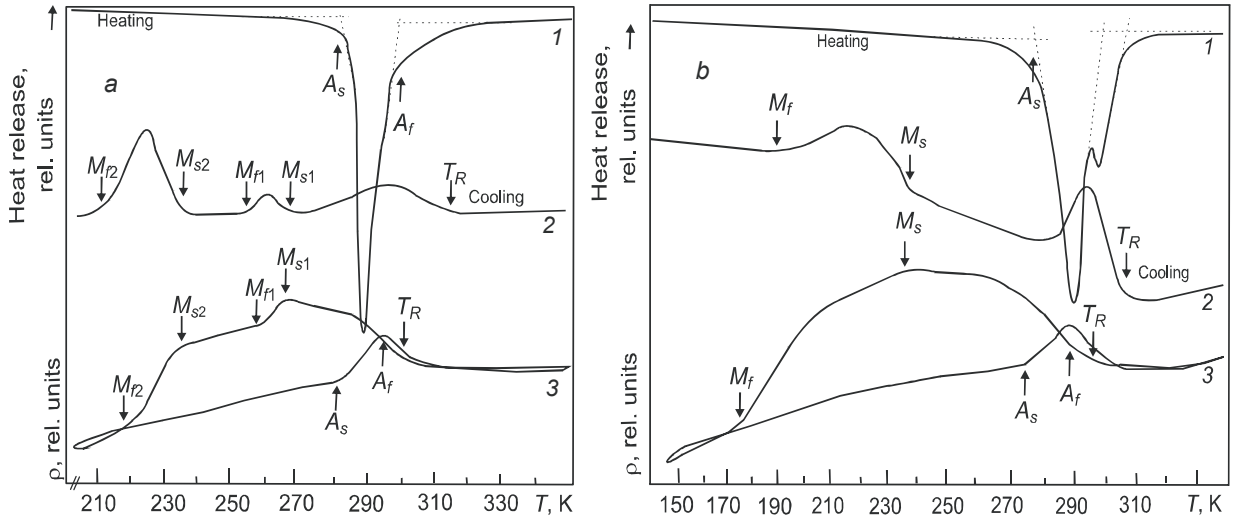

Fig. 1. DSC curves (curves *1*, *2*) and a ρ(*T*) plot (curve *3*) from $Ti_{49.0}Ni_{51.0}$ single crystals after aging at 823 K, 1.5 h under slow heating and cooling (15 ± 1) K/min condition (*a*) and after aging at 773 K, 1 h under slow heating and cooling (15 ± 1) K/min condition (*b*).

2. EXPERIMENTAL RESULTS AND DISCUSSION

No MSMTs were experimentally found out in Ti–Ni (50.8 at.% ≤ C_{Ni} ≤ 51.0 at.%) single crystals for all aging modes T = 673–823 K for t = 1–1.5 h in helium with fast heating followed by quenching into water: the direct MT occurred in two stages only *B*2–*R* and *R*–*B*19′ [15]. On the other hand, aging at 823 K, t = 1.5 h in a vacuum setup with slow cooling and heating (heating/cooling rate ~(15±1) K/min) of $Ti_{49.0}Ni_{51.0}$ single crystals was found to result in MSMTs occurring in them. Following this aging treatment, a two-step drop in the electrical resistance was observed in the ρ(*T*) plot, and three peaks of heat release in the DSC curves during cooling (Fig. 1*a*). The first high-temperature peak of heat release in the DSC curves coincides with the increase in electrical resistance in the ρ(*T*) plot, which is well known [1–4] to correspond to a *B*2–*R* MT. At the temperatures in the vicinity of the first peak in the DSC curves, a TEM examination reveals the formation of an *R*-phase around the particles, which disappears after heating of the foil.

The early first peak in the DSC curve during cooling coincides with the onset of the drop of electrical resistance in the ρ(*T*) plot, while the early third DSC peak coincides with a bend in this stage. We can therefore assume that the second and third peaks are associated with the *R*→*B*19′ MT (Fig. 1*a*). The amplitude of the second peak is low compared to that of the third, which suggests a small volume fraction of the material undergoing an *R*–*B*19′ MT at a higher temperature M_{s1} compared to the fraction of the crystal within which an *R*–*B*19′ MT occurs at a lower temperature M_{s2}. the temperature range of the *R*–*B*19′-transformation, corresponding to the second peak of heat release, is found to be $\Delta_1^1 = M_{s1} - M_{f1}$ = 12–15 K, while for the third peak it is $\Delta_1^2 = M_{s2} - M_{f2}$ = 20–25 K. Thus, a direct *R*→*B*19′ MT in these crystals occurs in a wide temperature interval $\Delta_1 = M_{s1} - M_{f2}$ = 50–60 K. A reverse *B*19′–*B*2 MT in $Ti_{49.0}Ni_{51.0}$ single crystals aged at 823 K, 1.5 h under slow heating and cooling conditions occurs in a single stage within a narrow temperature interval $\Delta_2 = A_f - A_s$ = 17–18 K (Fig. 1*a*).

Aging of $Ti_{49.0}Ni_{51.0}$ single crystals at 773 K, t = 1 h under slow heating/cooling conditions does not give rise to MSMTs (Fig. 1*b*). The DSC curves from these single crystals contain two heat-release peaks. The first high-temperature peak corresponds to a *B*2–*R* MT. The second low-temperature peak has a complex structure that could be treated as a superposition of two peaks (Fig. 1*b*, curve *2*). The ρ(*T*) plot within this temperature interval is characterized by a lengthy stage of a direct *R*–*B*19′ MT with $\Delta_1 = M_s - M_f \approx$ 60 K and a different tilt of the ρ(*T*) curve, which is indicative of a different intensity of the MT development within this temperature interval (Fig. 1*b*, curve *3*). The reverse

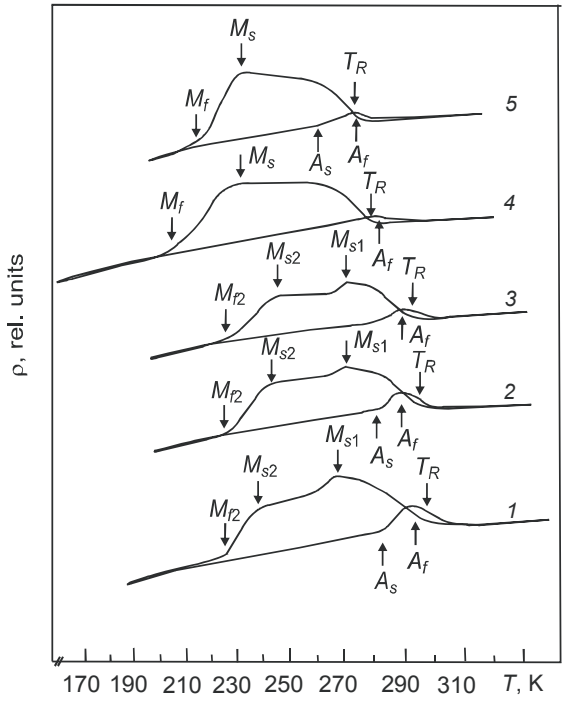

Fig. 2. The ρ(T) plots for $Ti_{49.0}Ni_{51.0}$ single crystals aged at 823 K for different aging periods: t = 1.5 h and slow heating/cooling rate (15 ± 1) K/min (curve *1*), t = 3.0 h (curve *2*), t = 8.5 h (curve *3*), t = 13.5 h (curve *4*), t = 18.5 h (curve *5*); aging (curves *2*–*5*) was followed by cooling in air for 10 min.

transformation occurs in a narrow temperature interval $\Delta_2 < 25$ K, despite the fact that the peak of heat absorption in the DSC curves consists of two distinct peaks corresponding to the *B*19′–*R*- and *R*–*B*2-transformations. During aging at a lower temperature 673 K for 1–1.5 h under conditions of slow heating/cooling (15 ± 1) K/min, no MSMTs were observed in the $Ti_{49.0}Ni_{51.0}$ single crystals under study. There are none in $Ti_{49.7}Ni_{51.3}$ single crystals aged at 773 K, as shown in [19].

Figure 2 clearly demonstrates that aging of $Ti_{49.0}Ni_{51.0}$ single crystals undergoing MSMTs (curve *1*) at 823 K during longer that 13.5 h, followed by cooling in air, does not result in any MSMTs (Fig. 2, curves *4* and *5*). It should be noted that irrespective of the fact whether the direct MT occurs in one stage or in two, the reverse MT in the aged TiNi single crystals is realized within a narrow temperature interval $\Delta_2 < 25$ K.

The investigations performed in [19], using single crystals $Ti_{49.7}Ni_{51.3}$ aged at 823 K in free state and under a compressive load of 50 MPa, support the observation that there are no MSMTs in the early stage of aging $t < 1$ h and for longer aging periods $t > 13.6$ h, and irrespective of the number of stages of the direct MT, the reverse MT occurs in a single stage within a narrow temperature interval $\Delta_2 < 25$ K.

Thus, in the absence of the effect of grain boundaries on the distribution of disperse particles in the aged $Ti_{49.0}Ni_{51.0}$ single crystals an MSMT is likely to occur under a certain aging condition, specifically, at T = 823 K for t = 1.5–7 h and slow heating and cooling rates (15 ± 1) K/min. Longer aging of Ti–Ni single crystals at T = 823 K, $t > 13.5$ h or aging at T = 673–823 K for t = 1–1.5 h followed by quenching in water do not give rise to any MSMTs, independent of the cooling rate [15, 16].

According to TEM examinations of the $Ti_{49.0}Ni_{51.0}$ single crystal specimens aged at 823 K for 1 h followed by quenching [15] and slow-heating/cooling (Fig. 3), the differences in their microstructure are hard to differentiate. In both cases there is precipitation of disperse Ti_3Ni_4 particles with d ranging from 370 to 450 nm, whose volume fraction is $f \sim 9.0\%$ and interparticle spacing lies within $\lambda = (370 \pm 30)$ nm. In $Ti_{49.0}Ni_{51.0}$ single crystals aged at 823 K for 1.5 h both in the case of fast heating and quenching in water and slow heating/cooling, the particle – matrix interface could

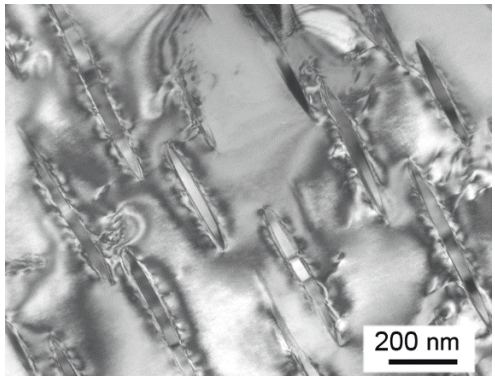

Fig. 3. Microstructure of $Ti_{49.0}Ni_{51.0}$ single crystals after aging at 823 K, t = 1.5 h under slow heating/cooling (15 ± 1) K/min.

act as the site of preferred nucleation of the $B19'$-martensite crystals due to the presence of local elastic stress fields $<\sigma_G>$ from the particles and/or the presence of a region depleted in Ni around the particles. Then the R–$B19'$ MT in the crystals aged under slow heating/cooling (Fig. 1*a*) discontinues at $T = M_{f1}$ and resumes only under further cooling down to $T = M_{s2}$, while in single crystals aged under fast heating followed by quenching, the R–$B19'$ MT is evolving continuously [15] though with a different intensity of martensite crystal formation.

A decrease in the aging temperature down to 773 K, a reduction in the Ti_3Ni_4 particle size to d = (100 ± 10) nm and a smaller interparticle spacing λ = (100 ± 10) nm compared to the case of $Ti_{49.0}Ni_{51.0}$ single crystals aged at 823 K resulted in a situation without MSMTs. This corresponds to the experimental data obtained in [19], which reports that MSMTs in the aged Ti–Ni crystals could be observed if the interparticle spacing is more than $\lambda > 200$ nm. According to the authors of [19], the absence of MSMTs in Ti–Ni poly- and single crystals in the early stage of aging under conditions of precipitation of disperse Ti_3Ni_4 particles measuring up to 100 nm and with the interparticle spacing being $\lambda < 100$ nm is associated with overlapping of both the elastic stress fields generated by the particles and the regions depleted in Ni.

In the overaged state at 823 K, $t > 13.5$ h, Ti_3Ni_4 particles measuring more than 600 nm can lose their coherence, which corresponds to relaxation of internal stresses from the particles and formation of dislocations at the particle–matrix interface [1, 2]. The relaxation of the local elastic stresses from the particles and the uniform distribution of Ni because of lengthy aging ensure that there is no high-temperature stage of the R–$B19'$ MT, which is associated with the development of an MT in the vicinity of the particles, thus no MSMT is observed (Fig. 2, curves *4* and *5*).

In order to model aging conditions in a vacuum setup, we performed an investigation of evolution of thermoelastic MTs in $Ti_{49.0}Ni_{51.0}$ single crystals following a two-stage aging processing – aging at 823 K followed by aging at a lower temperature and vice versa. According to the data reported in [15], aging of $Ti_{49.0}Ni_{51.0}$ single crystals at 673 K, 1 h gives rise to precipitation of Ti_3Ni_4 particles measuring 25–30 nm, which prevents the development of thermoelastic MTs and results in a lower MT temperature compared to the quenched crystals and those aged at a higher temperature. It could be therefore expected that aging at 823 K, 1.5 h and followed by aging at 673, 1 h might result in a bimodal particle distribution: in the spacings between large Ti_3Ni_4 particles measuring ~400 nm, provided a high concentration of N, fine Ti_3Ni_4 particles can form measuring 25–30 nm in size. Nonetheless, no MSMTs are observed in $Ti_{49.0}Ni_{51.0}$ single crystals in the case of this aging mode (Fig. 4). On the other hand, aging first at high temperature, 823 K, 1.5 h, and then a lower temperature, 573–623 K, 1 h, results in multiple sections (MSMTs) appearing in the $\rho(T)$ plot (Fig. 4, curve *3*).

It is assumed that given an excessive concentration of Ni in the space between large Ti_3Ni_4 particles measuring ~400 nm, fine concentration inhomogeneities rich in Ni would be formed, which were defined in [3] as equiaxial β'-phase 3–5 nm particles isostructural with respect to the matrix. One cannot entirely rule out possible precipitation of disperse Ti_3Ni_4 particles less than 10 nm in size in these regions, which requires additional studies.

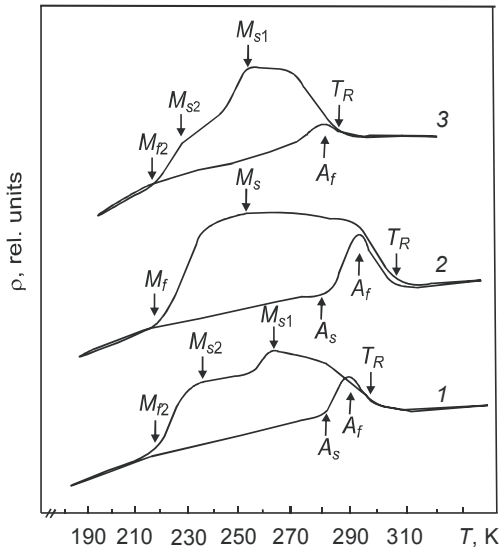

Fig. 4. The ρ(*T*) plots for $Ti_{49.0}Ni_{51.0}$ single crystals under different aging modes: aging at 823 K, *t* = 1.5. h aith slow heating/cooling (15 ± 1) K/min (I) (curve *1*), (I) + aging at 673 K, *t* =1 h, cooling in air for 10 min (curve *2*), (I) + aging at 573 K, *t* =1 h, cooling in air for 10 min (curve *3*).

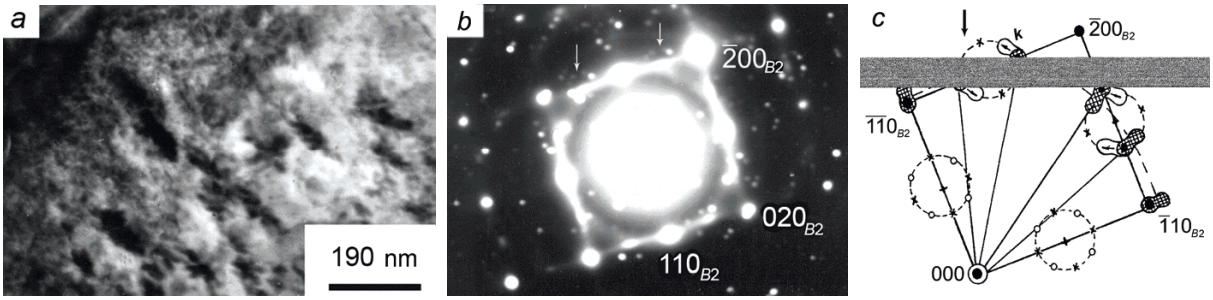

Fig. 5. Microstructure of $Ti_{49.0}Ni_{51.0}$ single crystals at 623 K, 1 h: bright-field image (*a*) and the respective microdiffraction pattern, zone axis $[001]_{B2}$ (*b*), and schematic distribution of diffusion scattering effects in the $(001)_{B2}$ cross section of the reciprocal lattice (*c*) [3].

Such types of noise in the electron microscopy contrast as ripple or tweed patterns are observed both in the bright-field (Fig. 5*a*) and dark-field images [3]. Moreover, the microdiffraction patterns exhibit additional diffusion scattering outside the Bragg reflections, which differs from the well-known pre-martensitic effects (strands and satellites along the <110>- and <112>-directions of the reciprocal lattice). Figure 5*b* presents an example of such a diffraction pattern with the $[001]_{B2}$ zonal axis and a schematic distribution of the diffuse scattering effects in Ti–Ni crystals in the stage of precipitation of β′-phase particles (Fig. 5) [3]. Thus, MSMTs are observed in Ti–Ni single crystals containing coarse disperse Ti_3Ni_4 particles measuring 400– 460 nm and fine disperse particles of the β′-phase precipitating between coarse particles under condition of slow heating/cooling and/or low-temperature aging at $T \leq 623$ K.

Relying on the examinations of microstructure of Ti–Ni single crystals aged at 823 K, *t* = 1.5 h under slow heating/cooling (Fig. 6*a–c*), we can assume the development of a direct *R–B*19′ MT to occur in a few stages via a scheme (Fig. 6*d*) developed in [10]. Figure 6*d* shows a schematic particle and the respective stress field. The local elastic stresses generated by the particles are maximum along the normal to the habitus plane of the particle anf quickly decrease with increasing *r* from the particle in proportion to $\sim 1/r$ [10].

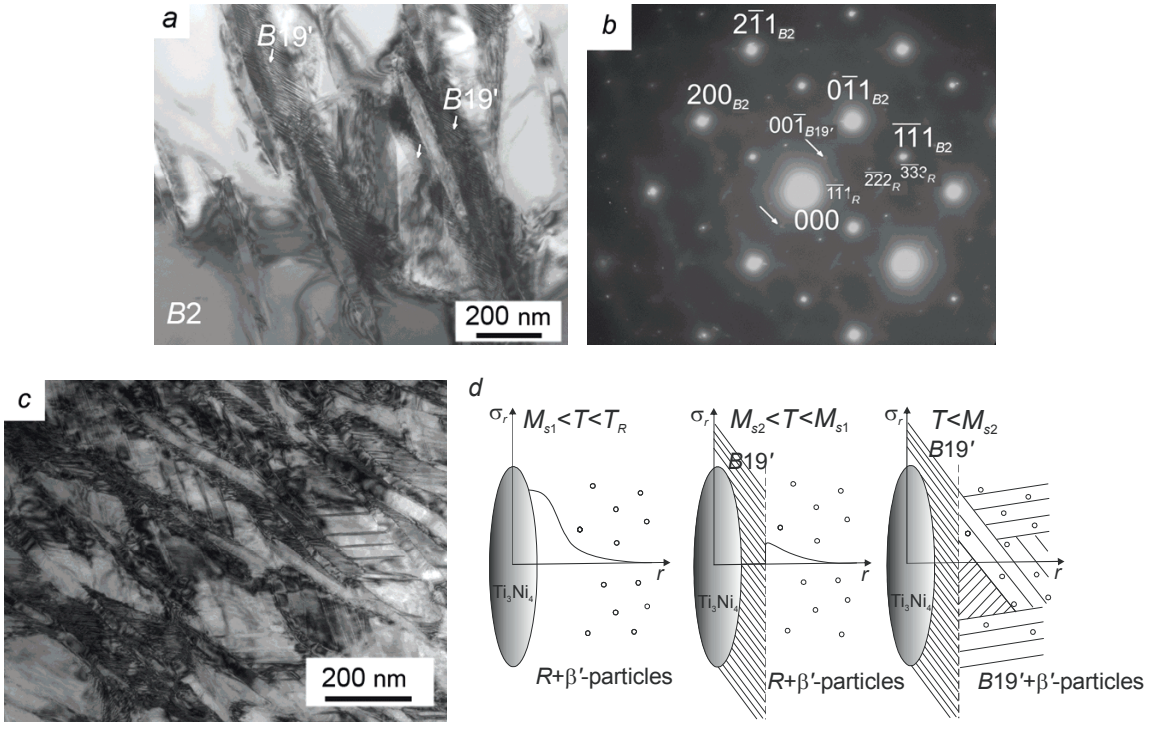

Fig. 6. Microstructure of the *B*19′-martensite: bright-field image of formation of the *B*19′-martensite in the vicinity of Ti_3Ni_4 particles in $Ti_{49.2}Ni_{50.8}$ single crystals aged without any loading at 823 K, 1.5 h (density of twins in the crystals of *B*19′-martensite $\rho_{tw} \sim 11.1 \cdot 10^{16}$ m^{-2}) (*a*), microdiffraction pattern for (*a*), zone axis $[011]_{B2} \parallel [011]_R \parallel [010]_{B19'}$ (*b*), bright-field image demonstrating different density of twins in crystals of the *B*19′-martensite near Ti_3Ni_4 particles (ρ_{tw} ~$11.1 \cdot 10^{16}$ m^{-2}) and in the interparticle spacing ($\rho_{tw} \sim 0.9 \cdot 10^{16}$ m^{-2}) in $Ti_{49.2}Ni_{50.8}$ single crystals aged at 823 K, 1.5 h under compressive loading (*c*) and a schematic development of a *R*–*B*19′ MSMT in the aged Ti–Ni single crystals (*d*).

At $M_{s1} < T < T_R$, the matrix is in the *R*-phase. Under cooling down to the temperature $M_{s2} < T < M_{s1}$, the *B*19′-martensite is the first to nucleate near the particles, which is favored by the local stress fields. In [10] it was demonstrated that the local fields, generated due to the differences in the lattice and matrix parameters, decrease with the distance from the particles at the particle – matrix interface and can become as low as 280 MPa. Thus, at $M_{s2} < T < M_{s1}$ a single variant of the *B*19′-martensite is produced, which has a maximum Schmidt factor in accordance with orientation of the internal stresses in the vicinity of large particles (Fig. 6*a*, *d*). Crystals of the *B*19′-martensite near the particles exhibit a high density of compound twins [100](001) (twin thickness ~3 nm, twin density $\rho_{tw} \sim 11.1 \cdot 10^{16}$ m^{-2}), as shown in Fig. 6*a*, *d* and is verified by the *in situ* electron microscopy investigations performed in [10, 19, 20]. It is well known [1, 2, 10] that a *B*2–*R* MT is characterized by low transformation entropy $\Delta S^{B2-R} =$ –0.219 J/(mol·K) and small lattice deformation $\varepsilon_0 \sim 1\%$, thus the method sensitivity does not allow the peaks in the DSC curves corresponding to the *B*2–*R* MTs to be differentiated. The β′-particles rich in Ni [3], which precipitate during slow cooling from 823 K and/or low-temperature aging at 523–623 K, give rise to a decrease in Ni concentration in the matrix between two large Ti_3Ni_4 particles but at the same time hinder the development of an MT and reduce the starting MT temperature M_s, compared to a single-phase matrix, both due to increased elastic and surface energies $|\Delta G_{\text{rev}}|$ of martensite crystals containing nanodisperse particles and higher resistance to the phase-boundary motion $|\Delta G_{fr}|$, and hence higher free non-chemical energy ΔG_{nonch} during the *R*–*B*19′ MT. Therefore, at $T = M_{f1}$ the transformation terminates. The second stage of the *R*–*B*19′ MT starts at the temperature M_{s2}, which corresponds to the

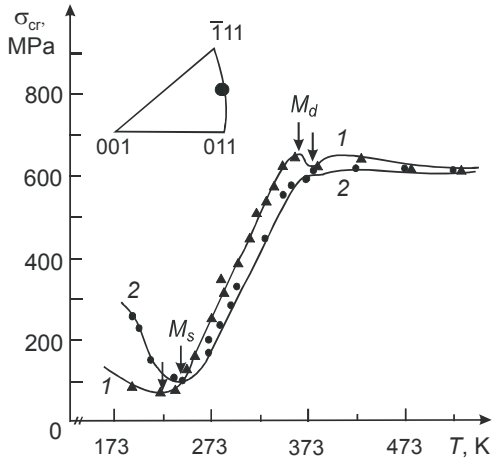

Fig. 7. Yield stress versus temperature under tensile loading for the [$\bar{1}$ 11] $Ti_{49.0}Ni_{51.0}$ single crystals: aged at 823 K, 1.5 h under fast heating followed by quenching in water (curve *1*), aged at 823 K, 1.5 h under slow heating/cooling (15 ± 1) K/min (curve *2*).

beginning of an MT in the regions near coarse disperse particles (Fig. 6*c*, *d*). There can be several variants of the *B*19'-martensite with a lower twin density (twin thickness ~15 nm) than in the vicinity of Ti_3Ni_4 particles (twin thickness ~3 nm), as shown in Fig. *c*, *d* and is supported by the literature data [19, 20]. This clarifies the fact that the *R*–*B*19′ MT occurs within two distinct steps corresponding to an internal-stress-induced transformation near large Ti_3Ni_4 particles measuring $d \sim 400$ nm and a transformation in unstressed regions of the material containing the fine disperse β′-phase particles isomorphic with respect to the matrix.

In Ti–Ni single crystals, aged at 823 K, 1.5 h under fast heating followed by quenching in water, no particles of the β′-phase precipitate in the space between large particles, and the *R*–*B*19′ MT occurs in a single stage. This happens notwithstanding the fact that coarse disperse Ti_3Ni_4 particles measuring ~400 nm, which are observed in these single crystals, also serve as the sites of preferred nucleation of the *R*- and *B*19′-martensite [3, 10].

The temperature dependence of critical stresses $\sigma_{cr}(T)$ of the martensitic shear and the yield stress of the high-temperature phase for $Ti_{49.0}Ni_{51.0}$ single crystals, aged at 823 K, 1.5 h followed by quenching in water and under conditions of slow heating/cooling at the (15 ± 1) K/min, is presented in Fig. 7. The minimum in the $\sigma_{cr}(T)$ curve for single crystals undergoing MSMTs coincides with the MT starting temperature M_{s2} in the bulk of the material. The data presented in the $\rho(T)$ plot and DSC curves for the aging condition under slow heating and cooling suggest that the starting MT temperature in the bulk of the material M_{s2} is 15–20 K higher than the M_s temperature in the crystals aged with fast heating and subsequent cooling in water. This might be due to a lower concentration of Ni in the matrix after aging under slow heating/cooling in contrast to the case of fast-quenched crystals. Aging at 823 K, 1.5 h under slow heating and cooling slightly improves strength properties of the *B*2-phase by 20–50 MPa, while the slope ratio $\alpha = d\sigma_{cr}/dT$ and the MT temperature interval under loading $\Delta T_\sigma = M_d - M_s$ do not change in contrast to those of the $Ti_{49.0}Ni_{51.0}$ crystals aged at 823 K, 1.5 h with fast heating and quenching in water (Fig. 7). Thus, the difference in the heating and cooling mode during aging does not appreciably affect the behavior of the $\sigma_{cr}(T)$ plot at $T > M_s$. On the other hand, at $T < M_s$ for single crystals aged under slow heating/cooling the (resolved) critical stresses $\sigma_{cr}(198\ \text{K}) = 230$ MPa (Fig. 7, curve *2*), which is nearly three times higher than $\sigma_{cr}(198\ \text{K}) = 80$ MPa for the single crystals aged under fast heating and quenching in water (Fig. 7, curve *1*). A sharp increase of the $\sigma_{cr}(T)$ plot with decreasing temperature at $T < M_s$ could be an indirect indication of precipitation of fine β′-particles in $Ti_{49.0}Ni_{51.0}$ single crystals aged under slow heating/cooling. It is the fine β′-phase particles which cause an MSMT and considerably increase the friction force during twin-boundary motion in *B*19′-martensite under loading, which results in a sharp increase in σ_{cr} at $T < M_s$.

A reverse *B*19′–*B*2 MT in Ti–Ni single crystals, undergoing an MSMT under cooling conditions, is not divided into stages and occurs in a narrow temperature interval $\Delta_2 < \Delta_1$, as is the case for Ti–Ni single crystals aged at 673–

823 K with fast quenching in water [15]. In contrast, no such peculiarity of MT evolution is observed in single-phase Ti–Ni crystals and $\Delta_1 = \Delta_2 \sim 30$ K [15]. The physical reason for the non-symmetrical temperature intervals of MTs ($\Delta_2 < \Delta_1$) and the temperature hysteresis ($\Gamma_2 = A_s - M_f$ higher than $\Gamma_1 = A_f - M_s$) in the aged Ti–Ni crystals consists in the fact that crystals of the *B*19′-martensite exhibit a high density of geometrically necessary twins along the $(001)_{B19'}$ planes, which are generated to ensure compatibility of the martensitic deformation of the matrix and the elastic deformation of the Ti_3Ni_4 particles (Fig. 6*a*, *b*). For the reverse transformation to start, the energy barrier associated with de-twinning of the martensite has to be overcome and, hence, a considerable overheating $\Gamma_2 > \Gamma_1$has to be achieved. Further evolution of the reverse transformation follows an explosive kinetics path at a low value of Δ_2 due to re-activation of the elastic and surface energies during de-twinning of the *B*19′-martensite crystals.

SUMMARY

We have observed MSMTs in $Ti_{50.0-x}Ni_{50.0+x}$ (x = 0.8–1.0 at.%) single crystals aged at 823 K for 1.5 h at the heating/cooling rates 14–16 K/min and after stepwise aging at 823 K for 1.5 h + 573–623 K within 1–1.5 hours. The experimental data reported in this work suggest that the conditions necessary for MSMTs to be observed in the Ti–Ni crystals are as follows: first, the presence of disperse Ti_3Ni_4 particles about 400 nm in diameter. The particle – matrix interfaces during precipitation of such particles are the preferred sites of nucleation of crystals of the *B*19′-martensite due to the presence of local stress fields and/or a region depleted in Ni in the vicinity of these particles. Second, the presence of large interparticle space $\lambda > 200$ nm, which ensures nucleation of the *B*19′-martensite crystals and their growth in between the particles. Third, precipitation of fine disperse β′-phase particles isostructural with respect to the *B*2-matrix under conditions of slow cooling and/or low-temperature aging at 523–623 K, 1 h in the regions between Ti_3Ni_4 particles ~400 nm in diameter, which prevents the development of an *R*–*B*19′ MT. As a result, the *R*–*B*19′ MT is divided into two stages: the high-temperature stage at $T = M_{s1}$ is associated with the *R*–*B*19′-transformation under the action of local field stresses in the volume surrounding disperse Ti_3Ni_4 particles measuring 400–430 nm, and the low-temperature stage at a lower temperature $T = M_{s2}$ – with the transformations in the spaces between large particles containing the β′-phase particles isomorphic with respect to the matrix. Despite the stage-like character of the direct *B*2–*R*–*B*19′ MT in the aged Ti–Ni single crystals, the reverse *B*19′–*B*2-transformation is not divided into stages and occurs in a narrow temperature interval $\Delta_2 < \Delta_1$ due to reactivation of the elastic and surface energies under conditions of de-twinning of geometrically necessary twins along the (001) planes of the *B*19′-martensite crystals, which are generated in order to maintain compatibility of martensitic deformation of the matrix and elastic deformation of the Ti_3Ni_4 particles. The presence of MSMTs in the aged Ti–Ni single crystals does not affect the level of critical stresses of martensite formation at $T > M_s$, but gives rise to a threefold increase in the critical stresses to ensure twin boundary motion in the *B*19′-martensite at $T < M_s$ in contrast to the Ti–Ni single crystals aged under the same mode and subsequently quenched in water, which do not undergo any MSMTs.

The results have been obtained while performing an assignment set by the RF Ministry of Science, TOR No. 16.1346.

REFERENCES

1. K. Otsuka and C. M. Wayman, Shape Memory Materials, Cambridge University Press (1998).
2. K. Otsuka and X. Ren, Prog. Mater. Sci., **50**, 511–678 (2005).
3. V. G. Pushin, S. D. Prokoshin, R. Z. Valiev, et. al., Shape Memory Alloys Part I: Structure, Phase Transformations and Properties [in Russian], Ekaterinburg, UrB RAS (2006).
4. A. I. Lotkov and V. N. Grishkov, Russ. Phys. J., **33**, No. 2, 172–178 (1991).
5. H. Morawies, D. Stoz, T. Goryczka, and D. Chrobak, Scripta Mater., **35**, No. 4, 458–490 (1996).
6. S. H. Chang, S. K. Wu, and G. H. Chang, Scripta Mater., **52**, 1341–1346 (2005).
7. N. Resnina and S. Belyaev, J. Alloys and Compounds, **486**, 304–308 (2009).
8. J. Khalil-Allafi, X. Ren, and G. Eggeler, Acta Mater., **50**, 793–803 (2002).

9. S. V. Oleynikova, I. Yu. Khmelevskaya, S. D. Prokoshkin, and L. M. Kaputkina, in: Proc. Int. Conf. on Martensitic Transformations, Monterey, California (1992).
10. L. Bataillard, J.-E. Bidaux, and R. Gotthardt, Philos. Mag. A, **78**, No. 2, 327– 344 (1998).
11. J. Khalil-Allafi, A. Douhy, and G. Eggeler, Acta Mater., **50**, 4255–4274 (2002).
12. G. Fan, W. Chen, S. Yang, *et al*., Acta Mater., **52**, 4351–4362 (2004).
13. B. Karbakhsh Ravari, S. Farjami, and M. Nishida, Acta Mater., **69**, 17–29 (2014).
14. Z. Yang and D. Schryvers, Micron, **37**, 433–441 (2006).
15. E. Yu. Panchenko, Yu. I. Chumlyakov, I. V. Kireeva, *et al*., J. Phys. Met. Metallogr., **106**, No. 6, 577–589 (2008).
16. R. F. Hamilton, H. Sehitoglu, Y. Chumlyakov, and H. J. Maier, Acta Mater., **52**, No. 11, 3383–3402 (2004).
17. Yu. I. Chumlyakov, I. V. Kireeva, E. Yu. Panchenko, *et al*., Russ. Phys. J., **46**, No. 8, 811–824 (2003).
18. Yu. I. Chumlyakov, Yu. Panchenko, I. V. Kireeva, E. *et al*., J. Phys. IV, **112**, 799–802 (2003).
19. J. Michutta, Ch. Somsen, A. Yawny, *et al*., Acta Mater., **54**, 3525–3542 (2006).
20. J. F. Li, Z. Q. Zheng, X. W. Li, and S. C. Li, Mater. Sci. Eng. A, **523**, 207–213 (2009).